

Anodic Growth of Passive Layers on Steel Rebars in an Alkaline Medium Simulating the Concrete Pores

M. Sánchez^{a,b}, J. Gregori^a, M. C. Alonso^{b*,1}, J. J. García-Jareño^{a,1}, F. Vicente^{a,1}

^a Department of Physical Chemistry. University of Valencia. C/. Doctor Moliner 50.
46100 Burjassot. Spain

^b Institute of Construction Science “Eduardo Torroja”, CSIC, C/.Serrano Galvache 4.
28033 Madrid. Spain

Abstract

Electrochemical Impedance Spectroscopy (EIS) and Cyclic Voltammetry (CV) techniques have been used to study passive layers anodically grown on steel rebars in an aqueous alkaline solution simulating the electrolyte of the concrete pores. Nyquist diagrams recorded by EIS at the different stabilization potentials show a diffusional tail at low frequencies. The analysis of the impedance measurements has been made by means of an equivalent circuit with a Warburg component and within the framework of the Point Defect Model (PDM) theory. It is observed that the calculated concentration of vacancies is a function of the potential in accordance with the theoretical prediction of the PDM.

Keywords: Carbon Steel; Point Defect Model; Passive Layer; Alkaline Media; EIS

¹ ISE Member

* Corresponding autor. Tel. +34 91 302 04 40; fax. +34 91 302 07 00

Email adress: mcalonso@ietcc.csic.es

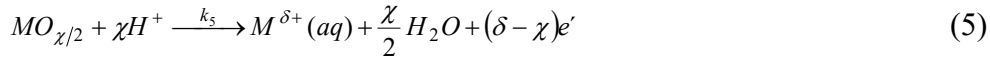
1. Introduction.

Steel rebars embedded in concrete are readily passivated due to the high alkaline pH of the aqueous electrolyte inside of the concrete pores. This passivation process allows the increase of the durability of concrete structures. Thus, the study of the steel passive state in alkaline media becomes important. Although several studies of steel passivity in alkaline media have been carried out [1–5], the knowledge about how is the growth of this passive layer is still uncertain. Several electrochemical techniques are employed to determine the corrosion processes of reinforcements embedded in concrete [2-3, 6-8]. Among them, Electrochemical Impedance Spectroscopy (EIS) and Cyclic Voltammetry (CV) are widely used in order to study the mechanism of passivation. Equivalent Electric Circuits, which simulate the electrical response of the system to an AC signal, are often employed to analyse the impedance measurements [9-11].

Mott-Schottky analysis has been extensively employed to characterize passive oxide films on metals, since passive layers formed under certain experimental conditions on transition metals show semiconductor behaviour [11-14]. However, a controversy about the valid conditions for the application of Mott-Schottky theory exists [15,16]. When this theory has been applicable, the passive film on Fe shows an n-type semiconductor behaviour [4,5].

On the other hand, the Point Defect Model (PDM) provides a microscopic and a mechanistic description for the passive film growth on metal surfaces. The PDM informs of the interpretation of the growth mechanism of passive layers on metal surfaces and also gives a description of the breakdown and dissolution mechanism of these layers [17-20]. PDM has been remarkably successful in accounting for the growth of passive films in different systems including nickel [21], titanium [22] or zinc [23].

Passive oxide films have been described to have a bilayer structure consisting of an *inner layer*, named “barrier layer”, that grows directly on the metal surface, and an *outer layer* precipitated via the hydrolysis of cations ejected from the inner layer [19,24,25]. According to the Point Defect Model (PDM) the barrier layer is described as a highly doped but graded defect semiconductor structure, in which vacancies are assumed to act as the electronic dopants [18,19,24]. A truncated version of the PDM, without considering the reactions for the generation and annihilation of cation vacancies, could be described by equations (1) to (5) [19,24,26]:

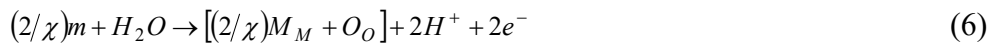


where the symbols are defined as follows: m (metal atom), $M_i^{\chi+}$ (metal cation interstitial), O_O (oxygen anion in anion site), $M^{\delta+}(aq)$ (metal cation in solution), $V_O^{\cdot\cdot}$ (anion vacancy), v_m (vacancy in metal phase).

During film growth, metal cation interstitials are produced at the metal/film interface, but are consumed at the film/solution interface. Likewise, anion vacancies are formed at the metal/film interface, but are consumed at the film/solution interface. Thus, under anodic polarization a net flow of oxygen vacancies from the metal/barrier layer interface to the barrier layer/outer layer interface and a net flow of metal cation interstitials in the reverse direction exist.

A spinel oxide (Fe₂O₃, Fe₃O₄ or related structure) has been reported [27,28] for passive films on Fe. An n-type semiconducting behaviour has been generally accepted for the passive film formed on Fe [29] and, according to the PDM, the dopants of this type of passive layers could be oxygen vacancies or cation interstitials [20]. Likewise, cation vacancies dope the film p-type [20].

The global effect of the movement of anion vacancies across the film leads to film growth according to the overall process defined by equation 6 [18,19]:



When the rate of the two non-conservative processes defined by equation (5) and equation (6) are equal [18,19] a steady-state is established.

The PDM theory takes into account the migration of point defects (vacancies) under the influence of the electrostatic field in the film, and also, the influence of concentration gradients within the passive film [18,19].

The aim of this work is to study the applicability of the PDM theory to the analysis of the electrochemical impedance for passive layers anodically growth on a steel rebar immersed in an alkaline solution simulating the concrete pores content. A truncated version of the PDM, defined by equations (1)-(5), has been considered in this work, without taking into account the processes related with the generation and annihilation of metal vacancies which dope the film p-type.

To consider the transport of vacancies within the potentiostatically electrogenerated passive layers different anodic stabilization potentials from the open circuit potential, an equivalent electric circuit containing a Warburg component has been considered to analyse the impedance diagrams. Since the thickness of the passive layer is finite, the transport impedance would be represented by a transmission line model [22], but, for high values of the time constant associated with the transport

process (large thickness of the layer or small diffusion coefficients), a Warburg element should be a good approximation for relatively high frequencies.

2. Experimental.

All the experiments have been carried out in a typical three electrodes electrochemical cell in a saturated $\text{Ca}(\text{OH})_2$ solution with the addition of 0.2 M KOH (pH = 13.2) which simulate the concrete pores aqueous content. The reference electrode was an $\text{Ag}|\text{AgCl}|\text{KCl}(\text{sat.})$ electrode but all the potentials in this work have been referred with respect to the Saturated Calomel Electrode (SCE). A rod of graphite ($\Phi=5\text{mm}$) was used as counter electrode. The working electrodes were made from a steel rebar ($\Phi=6\text{mm}$) covered with a cathoretic paint and embedded in epoxy resin. A photograph of the working electrode has been included in figure 1. The geometric area was $A = 0.28 \text{ cm}^2$. Before each experiment the steel surface was polished with emery paper, degreased and washed with double deionised water, to ensure the same superficial state before each measurement. The three electrodes were placed into a polyethylene cell, suitable for this high alkaline pH.

<Figure 1>

For impedance measurements the potential was controlled with a potentiostat-galvanostat 273A EG&G PAR and the impedance spectra were recorded with the help of a lock-in amplifier 5210 EG&G PAR. Impedance measurements were taken at different potentials (included in table 1) in the anodic direction from the corrosion potential since the anodic potentials enhance the rebar passivation. A stationary stage of layer growth was considered, applying a stabilization potential for 60 minutes before each impedance plot was obtained at this stabilization potential. All tests have been performed without stirring the electrolyte. The impedance measurements were carried out in the frequency range [10^5 to 10^{-2}] Hz and the amplitude of the harmonic potential

perturbation was 10 mV r.m.s. All the measurements were carried out at constant and controlled temperature $T = 298 \text{ K}$ under aerated conditions. All the impedance measurements have been performed under the same conditions. The fitting of experimental impedance data to the proposed equivalent circuit was carried out by means of a non-linear least squares procedure based on the Marquardt algorithm for function optimization [30,31].

Cyclic voltammetry measurement was obtained without stirring the working electrode, at constant and controlled temperature ($T = 298 \text{ K}$), in the $[-0.95 \text{ to } 0.75] \text{ V}_{\text{SCE}}$ potential window. Moreover, the initial potential $E_i = -0.95 \text{ V}_{\text{SCE}}$ was applied for 180 s before recording the voltammetric curve. Both in the anodic and in the cathodic scans the sweep rate was 0.5 mV/s .

3. Results and discussion.

The cyclic voltammetric curve for the steel rebar, obtained after the complete cycle is finished, has been represented in figure 2.

<Figure 2>

Although an increase of the anodic current density values in the potential range $[-0.6, -0.35] \text{ V}_{\text{SCE}}$ of the anodic scan has been observed, no clear anodic peaks have been distinguished. Previous studies in similar conditions [3] have identify in this potential range different oxidation peaks. However, the more relevant for present work is the passive observed in the potential range $[-0.35 \text{ to } 0.35] \text{ V}_{\text{SCE}}$, in agreement with previous research [3]. Within this plateau, a constant residual current density, that defines the steady state current density, is measured, $i_{ss} \approx 5.5 \cdot 10^{-6} \text{ A/cm}^2$.

In figure 3, several electrochemical impedance spectra, recorded at the different stabilization potentials located on the anodic branch in the passive potential range $[-0.35 \text{ to } 0.35] \text{ V}_{\text{SCE}}$ of the voltammetric curve (figure 2), are given.

<Figure 3>

An increase of the impedance values at low frequencies with the more anodic stabilization potential is observed. The shape of the recorded impedance spectra is consistent with those found in the literature under similar experimental conditions of stabilization time of the applied potential [4,5].

The compliance of the system with the constraints of the Linear Systems Theory (LST) has been confirmed by Kramers-Kronig transformation. Thus, the steady-state of the system during impedance measurements is assured [32,33]. The application of Kramers-Kronig transformation to the measured impedance spectra shows a good agreement between experimental and transformed real and imaginary components of the electrode impedance (figure 4), confirming the compliance of the system with the Linear Systems Theory. Therefore, the steady state of the system during the impedance measurements is assured.

<Figure 4>

A hierarchically distributed equivalent circuit, reproduced in figure 5a, has been reported [4,10] to model the behaviour of steel in alkaline media.

<Figure 5>

The values of the fitting for the passive elements of the considered equivalent circuit (figure 5a) are listed in table 1 as a function of the stabilization potential.

<Table 1>

No appreciable changes in the charge transfer resistance defined by R_1 are detected. The impedance of the CPE element is defined as $Z_{CPE} = 1/C(j\omega)^\alpha$ and the interpretation of this element depends on α value [33]. The obtained values for the exponent α_2 are close to 0.5 at all the stabilization potentials. Consequently, the interpretation of the CPE₂ element as a capacitance would be questionable. Contrarily,

the obtained $\alpha_2 = 0.5$ values are typical of a Warburg element which represent a diffusion control at low frequencies. Then, the experimental data should be fitted with the equivalent electric circuit of figure 5b, including a Warburg component [21]. In table 2 the values for the passive elements obtained from the fitting procedure to this equivalent circuit has been included.

<Table 2>

Over the whole explored potential range $[-0.35 \text{ to } 0.35] V_{SCE}$, similar values with small variations for the charge transfer resistance defined by R_1 are observed. This result is consistent with the absence of anodic peaks in this potential range registered by the voltammetric curve (figure 2) and also with the nearly constant value measured for i_{ss} . The observed low-intensity current plateau should be associated with the thickening and structural changes of the electrogenerated passive film. Thus, a quick passivation of the steel rebar, without current peaks seems to occur when is immersed in an alkaline medium and the experimental conditions used in present work.

Finally, α_1 values close to 0.9 are observed in all cases from table 2 indicating that an interpretation of the CPE_1 element as a capacitance should be acceptable. The variation of this capacitance with the potential is included in table 2.

When a steel rebar is immersed in the alkaline media simulating the aqueous content of the concrete pores, a stable passive layer, with semiconductor behaviour, is readily formed on the surface. The composition and protective character of this layer depend on the rebar potential [5,20].

The capacitance associated with CPE_1 element of the equivalent circuit of figure 5b changes with the stabilization potential, as can be seen in table 2. This capacitance includes several contributions associated with the high frequency time constant, as are

the passive layer space-charge capacitance C_{SC} , related with the charge carriers containing in the oxide barrier layer, and the Helmontz layer capacitance C_H [4,13,20]:

$$\frac{1}{C_1} = \frac{1}{C_{SC}} + \frac{1}{C_H} \quad (7)$$

The values for C_H can be estimated from the EIS data obtained at the potential of the hydrogen evolution, at which the steel surface may be considered free of oxides. A value of $C_H = 110 \mu\text{F}/\text{cm}^2$ is obtained in these conditions. Then, C_{SC} values could be calculated from equation (7). The obtained values are represented in figure 6 in the form of Mott-Schottky plot.

<Figure 6>

From figure 6 is possible to establish a linear relationship between $1/C_{SC}^2$ and the applied potential in the $[-0.05, 0.25] \text{ V}_{\text{SCE}}$ potential range. Then, the application of the Mott-Schottky equation could be tempted:

$$\frac{1}{C_{SC}^2} = \frac{2}{eN_D \epsilon_r \epsilon_0} \left(E - E_{fb} - \frac{kT}{e} \right) \quad (8)$$

where e ($1.602 \cdot 10^{-19} \text{ C}$) is the electron charge, ϵ_0 ($8.8542 \cdot 10^{-12} \text{ F/m}$) is the permittivity of free space and ϵ_r ($= 12$) is the relative dielectric constant of Fe_2O_3 [34].

Applying the Mott-Schottky analysis [12-14] in this potential range, the effective donor concentration N_D and the flat band potential E_{fb} can be estimated. The donor concentration value $N_D = 8.1 \cdot 10^{21} \text{ cm}^{-3}$ obtained is slightly higher than that reported in literature [5,6,36], and the estimated value for the flat band potential $E_{fb} = -0.11 \text{ V}_{\text{SCE}}$ is more cathodic than the expected one [35]. Thus, Mott-Schottky analysis allows to obtain approximate values from Mott-Schottky but this results should be take with care, because only maintaining constant the film thickness, this analysis gives a valid relationship between the applied voltage and the capacitance measurements at high frequency [20,35].

Therefore, when the thickness of passive oxide films depend on the applied potential, the interpretation of the experimental data in terms of the Point Defect Model (PDM) [17-19] may be more appropriate than the Mott-Schottky analysis. PDM theory provides a microscopic and mechanistic description of the passive layers based on the existence and transport of point ionic vacancies through the barrier oxide layers [19-21], which would explain the presence of a transport tail at low frequencies in the impedance spectra of figure 3, and the use of a Warburg component in the electric equivalent circuit considered for modelling the EIS measurements obtained in the present work.

The transport impedance through a layer of finite thickness δ can be defined as [36]:

$$Z_{\delta} = \sigma \frac{th\sqrt{j\omega\tau_D}}{\sqrt{j\omega\tau_D}} \quad (9)$$

However, for relatively high frequencies, the following approximation could be considered [37]:

$$\lim_{\omega \rightarrow \infty} Z_{\delta} = \sigma \frac{(1-j)}{\sqrt{2\omega\tau_D}} \quad (10)$$

which defines the Warburg impedance. The frequency range for which this approximation is valid depends on the $\tau_D = \delta^2/D$ values, where δ represents generally the layer thickness and D the diffusion coefficient. For very low D values this frequency range is shifted towards lower values.

Also, the PDM considers that the film thickness at the steady state depends on the applied voltage by a linear dependency [19,21]. According to the PDM and the n-semiconductor behaviour of the Fe passive layer, the predominant vacancies would be oxygen vacancies or metal cation interstitials [19]. The present study is not able to distinguish between these two possibilities and, consequently, in the following

mathematical treatment the global concentration of vacancies, defined by C_V , has been considered. The concentration of the diffusing vacancies C_V within the film could be calculated from the Warburg coefficient σ , according to the equation [38]:

$$\sigma = \frac{R \cdot T}{n^2 \cdot F^2 \cdot \sqrt{2}} \cdot \frac{1}{C_V \cdot \sqrt{D_V}} \quad (11)$$

where σ is the Warburg coefficient ($\Omega \cdot \text{cm}^2 \cdot \text{s}^{-0.5}$) and D_V is the vacancy diffusion coefficient (cm^2/s) and the other symbols have their usual meaning. According to literature data [5], a value of $D_V \approx 7 \cdot 10^{-17} \text{ cm}^2/\text{s}$ has been considered. D_V value is probably too large, compared with that for a single crystal, since the barrier layer on iron comprises nano, columnar grains and hence has a large fraction of grain boundaries.

The donor concentration, N_D , could be estimated from the concentration of diffusing species multiplying by the Avogadro number ($N_A = 6.02 \cdot 10^{23} \text{ particles/cm}^3$) according to:

$$N_D = N_A \cdot C_V \quad (12)$$

The donor concentration N_D values, obtained as a function of the stabilization potential, have been represented in figure 7.

<Figure 7>

A continuous decrease in the vacancy concentration values with the increase of the applied potential has been observed. This fact can be related with a more protective character of the electrogenerated oxide layer at more anodic potentials. From figure 7 that a linear relationship between N_D and the stabilization potential in the $[-0.35 \text{ to } 0.25]$ V_{SCE} potential range can be deduced. It is interesting to observe that a theoretical prediction of the PDM implies that the following expression holds according to [20]:

$$N_D = \omega_1 \exp(-bE) + \omega_2 \quad (13)$$

where ω_1 , ω_2 and b are parameters related with the transport and electrical properties of the passive layer, and E represents the applied potential. For small values of $(-b \cdot E)$, the exponential could be approximated to a linear dependence and the following approximation is valid:

$$N_D = \omega_1(1 - b \cdot E) + \omega_2 \quad (14)$$

Under these conditions, a linear dependence for the vacancy concentration on the applied potential could be expected according to equation (14) and experimental results of present work are consistent with this hypothesis (figure 7).

Finally, according to the PDM, the steady-state current density value in the Fe passive state is nearly independent of potential [19]. In addition, $R_1 \cdot i_{ss}$ has also a constant value. Then, R_1 values must be potential independent in this case as is experimentally observed (Table 2) in the $[-0.35, 0.25]$ V_{SCE} potential range of the applied potential.

5. Conclusion.

The long term application (60 minutes) of an anodic stabilization potential causes the electric appearance of a low frequencies transport component in the recorded impedance spectra. Consequently, a Warburg element is included in the electric equivalent circuit used in the analysis procedure within the framework of the PDM theory. Our experimental results show a linear decrease of the donor concentration when the potential increases in good agreement with the theoretical consequences of the PDM. Moreover, a nearly potential independent charge transfer resistance is calculated which is consistent with the n-type semiconductor character of the passive layers on Fe since the oxygen vacancies are the predominant point defects in these experimental conditions. Consequently, PDM theory seems valid in order to interpret the EIS spectra

corresponding to the passive state of a steel rebar immersed in an alkaline medium simulating the concrete pores.

Acknowledgements

This work has been supported partially by the Spanish Environmental Ministry (project 6.1-210/2005/2-B). M. Sánchez and J. Gregori acknowledge their Fellowship from the Spanish Education Ministry (FPU program).. J. J. García-Jareño acknowledges his position (Program “Ramón y Cajal”) to the Spanish Science and Technology Ministry.

References

- [1] M. Stern, A.L. Geary, *J. Electrochem Soc.* 104 (1957) 56.
- [2] G.K. Glass, C.L. Page, N.R. Short, J.Z. Zhang, *Corros. Sci.* 39 (1997) 1657.
- [3] S. Joiret, M. Keddou, X.R. Nóvoa, M.C. Pérez, C. Rangel, H. Takenouti, *Cem. Conc. Comp.* 24 (2002) 7.
- [4] E.B. Castro, J.R. Vilche, *Electrochim. Acta* 38 (1993) 1567.
- [5] E.B. Castro, *Electrochim. Acta* 39 (1994) 2117.
- [6] C. Andrade, V. Castelo, C. Alonso, J.A. González, In: Chaker V, Editor. *Corrosion Effect of Stray Currents and the Techniques for Evaluating Corrosion of Rebars in Concrete*. ASTM STP 906. Philadelphia: American Society for Testing and Materials (1986) pp 43.
- [7] C.L. Page, K.W.J. Treadaway, P.B. Bamforth, *Corrosion of Reinforcement in concrete*. Elsevier Applied Science. London (1990).
- [8] N.S. Berke, V. Chaker, D. Whiting, *Corrosion Rates of Steel in Concrete*. ASTM STP 1065. Philadelphia (1990).
- [9] V. Feliú, J.A. Gonzalez, C. Andrade, S. Feliú, *Corros. Sci.* 40 (1998) 975.
- [10] C. Andrade, C. Alonso, M. Keddou, X.R. Nóvoa, H. Takenouti, *Cem. Conc. Res.* 27 (1997) 1191.
- [11] W.P. Gomes, D. Vanmaekelbergh, *Electrochim. Acta* 41 (1996) 967.
- [12] J. Sikora, E. Sikora, D.D. Macdonald, *Electrochim. Acta* 45 (2000) 1875.
- [13] G. Oskam, D. Vanmaekelbergh, J.J. Kelly, *J. Electroanal. Chem.* 315 (1991) 65.
- [14] M. Metikoš-Huković, S. Omanović, A. Jukić, *Electrochim. Acta* 45 (1999) 977.
- [15] C. Chen, B.D. Cahan, *J. Electrochem. Soc.* 129 (1982) 474.
- [16] C. da Fonseca, S. Boudin, M. da Cunha Belo, *J. Electroanal. Chem.* 379 (1994) 173.

- [17] C.Y. Chao, L.F. Lin, D.D. Macdonald, *Electrochem. Soc.* 128 (1981) 1187.
- [18] D.D. Macdonald, *J. Electrochem. Soc.* 139 (1992) 2395.
- [19] D.D. Macdonald, S. Biaggio, H. Song, *J. Electrochem. Soc.* 139 (1992) 3434.
- [20] E. Sikora, J. Sikora, D.D. Macdonald, *Electrochim. Acta* 41 (1996) 783.
- [21] D.D. Macdonald, R.Y. Liang, B.G. Pound, *J. Electrochem. Soc.* 12 (1987) 134.
- [22] Z. Tun, J.J. Noel, D.W. Shoesmith, *J. Electrochem. Soc.* 146 (1999) 988.
- [23] D.D. Macdonald, K. Ismail, E. Sikora, *J. Electrochem. Soc.* 145 (1998) 3141.
- [24] D.D. Macdonald, *Pure Appl. Chem.* 71 (1999) 951.
- [25] F. Vicente, J. Gregori, J.J. García Jareño, D. Giménez-Romero, *J. Solid State Electrochem.* 9 (2005) 684.
- [26] D. D. Macdonald, M. Al Rifaie,, R. Engelhardt, *J. Electrochem. Soc.* 148 (2001) B343.
- [27] A.J. Davenport, L. J. Oblonsky, M. P. Ryan, M. F. Toney, *J. Electrochem. Soc.* 147 (2000) 2162.
- [28] M. F. Toney, A. J. Davenport, L. J. Oblonsky, M. P. Ryan, C. M. Vitus, *Phys. Rev. Lett.* 79 (1997) 4282.
- [29] J. S. Kim, E. A. Cho, H. S. Kwon, *Corros. Sci.* 43 (2001) 1403.
- [30] J.R. Macdonald, *Solid State Ionics* 58 (1992) 97.
- [31] F. Vicente, J.J. García-Jareño,,A. Sanmatías (2000) *Procesos Electródicos del NAFIÓN y del Azul de Prusia sobre electrodo transparente de óxido de indio-estaño: un modelo de electrodo multicapa.* Moliner-40. Burjassot
- [32] P. Agarval, M.E. Orazem, L.H. Garcia-Rubio, *J. Electrochem. Soc.* 139 (1992) 1917.
- [33] J. R. Macdonald, *Impedance Spectroscopy. Emphasizing solid materials and systems.* Ed. J. R. Macdonald, John Wiley & Sons, (1987)

- [34] Handbook of Chemistry and Physics (1995) In: Lide DR (ed). CRC press. New York. p 12-53.
- [35] J.W. Schultze, M.M. Lohrengel, *Electrochim. Acta* 45 (2000) 2499.
- [36] J. P. Diard, B. Le Gorrec, C. Montella, “Cinétique Electrochimique”. Ed: Hermann. Paris. 1996. p. 247.
- [37] Z. Grubač, M. Metikoš-Huković, *J. Electroanal. Chem.* 565 (2004) 85.

Figure 1. Working electrode photograph. The exposed area was the transversal section of the rebar. The bottom part was employed for connecting the electrode.

Figure 2. Cyclic voltammetric curve for a steel rebar immersed in alkaline media simulating the pores concrete (saturated $\text{Ca}(\text{OH})_2$, 0.2 M KOH solution (pH = 13.2)). Sweep rate: 0.5 mV/s. [-0.95,0.75] V_{SCE} . T = 298 K.

Figure 3. Nyquist plots obtained at the different stabilization potentials indicated in the figure. Same experimental conditions than in figure 2. pH = 13.2. T = 298 K.

Figure 4. Kramers-Kronig transformation of the impedance diagram obtain after one hour of stabilization of the rebar at -0.35 V_{SCE} .

Figure 5a. Equivalent electric circuit with two hierarchically distributed time constants. R_0 is the electrolyte resistance. R_1 is associated with the charge transfer resistance and C_1 is assigned to the double layer capacitance. The second time constant R_2C_2 is related with the redox processes taking place in the passive layer. α_1 and α_2 model the Cole-Cole type dispersion of the time constants. $Z_{\text{CPE}} = 1/C(j\omega)^\alpha$. **Figure 5b.** Equivalent electric circuit considered for modelling the passive layer formed on the steel surface by stabilization at different potentials. The second CPE has been replaced by a Warburg element.

Figure 6. Mott-Schottky plots from C_{SC} calculated values by fitting to the equivalent circuit of figure 5b.

Figure 7. Evolution of vacancy concentration N_D with the stabilization potential for the passive layer grown over a steel rebar surface immersed in alkaline medium. pH = 13.2. T = 298K.

Table 1. Passive element values for the equivalent circuit of figure 5a obtained from the fitting procedure. Same experimental conditions than in figure 2.

Table 2. Passive element values for the equivalent circuit of figure 5b obtained from the fitting procedure. Same experimental conditions than in figure 2.